Carbon Dioxide Capture for Storage in Deep Geologic Formations – Results from the CO_2 Capture Project

Capture and Separation of Carbon Dioxide from Combustion Sources

Edited by

David C. Thomas
Senior Technical Advisor
Advanced Resources International, Inc.
4603 Clearwater Lane
Naperville, IL, USA

Volume 1

ELSEVIER
2005

Amsterdam – Boston – Heidelberg – London – New York – Oxford
Paris – San Diego – San Francisco – Singapore – Sydney – Tokyo

Elsevier Internet Homepage – http://www.elsevier.com
Consult the Elsevier homepage for full catalogue information on all books, major reference works, journals, electronic products and services.

Elsevier Titles of Related Interest

AN END TO GLOBAL WARMING
L.O. Williams
ISBN: 0-08-044045-2, 2002

FUNDAMENTALS AND TECHNOLOGY OF COMBUSTION
F. El-Mahallawy, S. El-Din Habik
ISBN: 0-08-044106-8, 2002

GREENHOUSE GAS CONTROL TECHNOLOGIES: 6TH INTERNATIONAL CONFERENCE
John Gale, Yoichi Kaya
ISBN: 0-08-044276-5, 2003

MITIGATING CLIMATE CHANGE: FLEXIBILITY MECHANISMS
T. Jackson
ISBN: 0-08-044092-4, 2001

Related Journals:
Elsevier publishes a wide-ranging portfolio of high quality research journals, encompassing the energy policy, environmental, and renewable energy fields. A sample journal issue is available online by visiting the Elsevier web site (details at the top of this page). Leading titles include:

Energy Policy
Renewable Energy
Energy Conversion and Management
Biomass & Bioenergy
Environmental Science & Policy
Global and Planetary Change
Atmospheric Environment
Chemosphere – Global Change Science
Fuel, Combustion & Flame
Fuel Processing Technology

All journals are available online via ScienceDirect: www.sciencedirect.com

To Contact the Publisher
Elsevier welcomes enquiries concerning publishing proposals: books, journal special issues, conference proceedings, etc. All formats and media can be considered. Should you have a publishing proposal you wish to discuss, please contact, without obligation, the publisher responsible for Elsevier's Energy program:

Henri van Dorssen
Publisher
Elsevier Ltd
The Boulevard, Langford Lane
Kidlington, Oxford
OX5 1GB, UK

Phone: +44 1865 84 3682
Fax: +44 1865 84 3931
E.mail: h.dorssen@elsevier.com

General enquiries, including placing orders, should be directed to Elsevier's Regional Sales Offices – please access the Elsevier homepage for full contact details (homepage details at the top of this page).

ELSEVIER B.V.
Radarweg 29
P.O. Box 211, 1000 AE Amsterdam
The Netherlands

ELSEVIER Inc.
525 B Street, Suite 1900
San Diego, CA 92101-4495
USA

ELSEVIER Ltd
The Boulevard, Langford Lane
Kidlington, Oxford OX5 1GB
UK

ELSEVIER Ltd
84 Theobalds Road
London WC1X 8RR
UK

First edition 2005

Library of Congress Cataloging in Publication Data
A catalog record is available from the Library of Congress.

British Library Cataloguing in Publication Data
A catalogue record is available from the British Library.

ISBN: 0-08-044570-5 (2 volume set)

Volume 1: Chapters 8, 9, 13, 14, 16, 17, 18, 24 and 32 were written with support of the U.S. Department of Energy under Contract No. DE-FC26-01NT41145. The Government reserves for itself and others acting on its behalf a royalty-free, non-exclusive, irrevocable, worldwide license for Governmental purposes to publish, distribute, translate, duplicate, exhibit and perform these copyrighted papers. EU co-funded work appears in chapters 19, 20, 21, 22, 23, 33, 34, 35, 36 and 37. Norwegian Research Council (Klimatek) co-funded work appears in chapters 1, 5, 7, 10, 12, 15 and 32.

Volume 2: The Storage Preface, Storage Integrity Preface, Monitoring and Verification Preface, Risk Assessment Preface and Chapters 1, 4, 6, 8, 13, 17, 18, 19, 20, 21, 22, 23, 24, 25, 26, 27, 28, 29, 30, 31, 32, 33 were written with support of the U.S. Department of Energy under Contract No. DE-FC26-01NT41145. The Government reserves for itself and others acting on its behalf a royalty-free, non-exclusive, irrevocable, worldwide license for Governmental purposes to publish, distribute, translate, duplicate, exhibit and perform these copyrighted papers. Norwegian Research Council (Klimatek) co-funded work appears in chapters 9, 15 and 16.

♾ The paper used in this publication meets the requirements of ANSI/NISO Z39.48-1992 (Permanence of Paper).
Printed in The Netherlands.

Carbon Dioxide Capture for Storage in Deep Geologic Formations, Volume 1
D.C. Thomas and S.M. Benson (Eds.)

Chapter 16

HYDROGEN TRANSPORT MEMBRANE TECHNOLOGY FOR SIMULTANEOUS CARBON DIOXIDE CAPTURE AND HYDROGEN SEPARATION IN A MEMBRANE SHIFT REACTOR

Michael V. Mundschau, Xiaobing Xie and Anthony F. Sammells

Eltron Research Inc., Boulder, CO, USA

ABSTRACT

A wide variety of dense hydrogen transport membranes were tested for feasibility of resisting a minimum differential pressure of 3.10 MPa while extracting hydrogen from simulated high pressure water gas shift reactors operating at 693–713 K at an absolute pressure of 3.20 MPa and containing a hydrogen partial pressure of 1.31 MPa. Membranes were tested for compatibility with operating conditions of commercial water gas shift catalysts of 90 wt% Fe_3O_4/10 wt% Cr_2O_3. Best hydrogen flux results were achieved using select metal membranes of Group IVB and VB elements (i.e. Nb, Ta, V, Zr) and their alloys coated with sub-micron thick layers of palladium. Free standing, unsupported disks, 1.6 mm in diameter, of select metals and alloys were found to resist the target differential pressure of 3.10 MPa with the target partial pressure of hydrogen of 1.31 MPa while producing a hydrogen flux of 2.1 mol m^{-2} s^{-1} at 713 K at essentially 100% selectivity. At a 3.10 MPa differential pressure and a hydrogen partial pressure of 2.90 MPa, a record hydrogen flux of 2.5 mol m^{-2} s^{-1} was achieved at 713 K. It was concluded that the metal membranes appear superior to other classes of membrane tested for separation of H_2 from CO_2 at high pressure and are the most likely to be cost effective in scaled up reactors. Because commercial water gas shift catalysts are likely to be deactivated by sintering when used above about 713 K, proton conducting ceramic membranes, which typically require temperatures well above about 1000 K, were eliminated from consideration. Thin films of palladium supported on various porous materials were evaluated. In order to minimize interfacial stress between palladium and its potential substrates, which can lead to the formation of dislocations and cracks, a computer search of approximately 50,000 compounds was performed to select materials which would crystallographically match the cubic symmetry of the palladium crystal lattice and which would match the crystallographic lattice constants at the atomic level within about 2%. It was also desired to match coefficients of thermal expansion from room temperature to a maximum anticipated operating temperature of 713 K. From a dozen porous compounds tested, $LaFe_{0.90}Cr_{0.10}O_{3-x}$ and $LaFeO_{3-x}$, performed best. However, it was concluded that, in general, hydrogen flux would likely be severely limited by gas phase diffusion of non-hydrogen gases through all conceivable thick porous supports needed to resist the extreme differential pressures, and that the predicted advantages of using micron-thin layers of palladium would be difficult to achieve. Also considered were dense cermets (ceramic metals) fabricated by sintering together powders of palladium or Group IVB–VB metals with ceramics which were lattice matched and matched for coefficients of thermal expansion. In the cermets tested, the hydrogen flux was predominantly through the metal phase (or along the metal ceramic phase boundaries) rather than through the ceramic phase. It was concluded that cost of scaled-up cermets of palladium might be prohibitive.

INTRODUCTION

As an alternative to burning fuels directly in air, all carbonaceous materials, in principle, can be steam reformed into a mixture of $H_2 + CO$. The CO can be further reacted with steam in water gas shift reactors operating at pressures up to 35 bar at 693–713 K to form CO_2 and additional H_2 [1]. If dense membranes were commercially available to separate CO_2 from H_2 in high pressure water gas shift reactors, the hydrogen extracted from one side of the membrane could be utilized as a clean fuel, and the CO_2, remaining at high pressure and undiluted by nitrogen on the retentate side of the membrane, would be in a very

concentrated form desirable for economic sequestration. Dense membranes have an advantage over porous membranes in that they possess essentially 100% selectivity for hydrogen.

In order for this Carbon Capture Project scenario to be feasible, low cost hydrogen transport membranes must be available which can withstand the harsh conditions of water gas shift reactors. Commercial reactors operate at absolute pressures up to 3.5 MPa in superheated steam with inlet temperatures between 613 and633 K and outlet temperatures between 693 and 713 K [1]. Assuming that the hydrogen fuel is desired a few atmospheres above ambient, membranes should resist a differential pressure of at least 3.1 MPa without rupture or leak, while maintaining a very high flux for hydrogen, preferentially with 100% selectively.

In this feasibility study, a wide variety of dense membrane materials were considered and tested in simulated water gas shift reactor conditions. Figure 1 shows schematically the major concepts of the common, dense, composite, hydrogen transport membranes. The CO_2 retentate side of the membrane facing the source of hydrogen is typically coated with a catalyst for the adsorption and dissociation of molecular hydrogen. Hydrogen is transported through the bulk of the dense membrane material in a dissociated form, typically as protons, H^+, and electrons, e^-, although transport as neutral hydrogen atoms or as hydride ions, H^-, cannot be ruled out for some membrane materials. The permeate side of the membrane facing the hydrogen sink is also typically coated with a catalyst for the recombination of dissociated hydrogen back into molecular hydrogen and for desorption of molecular hydrogen into a sweep gas of steam.

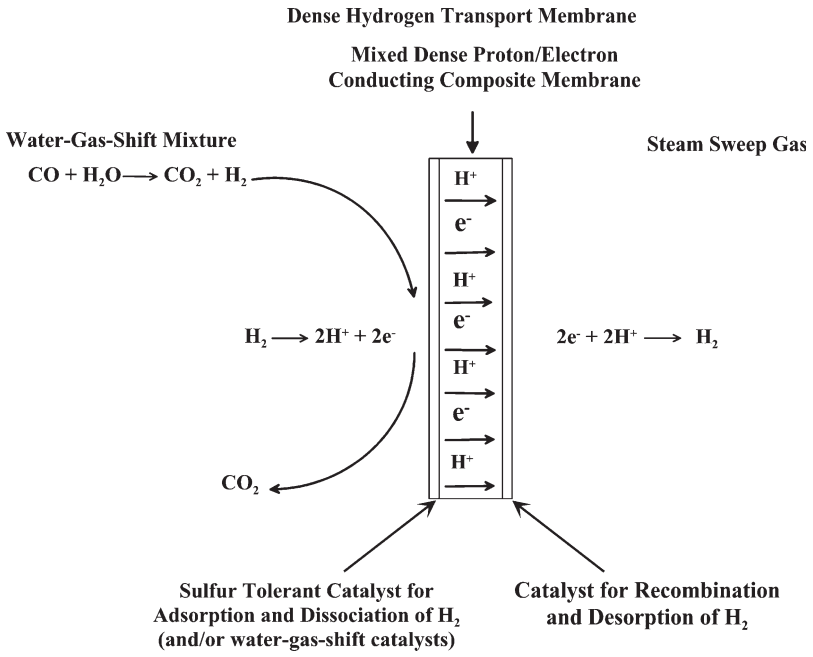

Figure 1: Schematic of dense hydrogen transport membranes.

Materials of high hydrogen permeability for the bulk membrane between the two layers of catalyst can include un-alloyed metals such as Nb, Ta, V and Zr, metal alloys of these elements, proton conducting ceramics, metal ceramic cermets, or other composites. Proton conducting ceramic oxides can include those with the perovskite crystal structure (see Figure 2) [2]. Dense cermets (ceramic metals) are fabricated by sintering together fine powders of metals and ceramics. Ceramics in cermets can include proton conducting oxides, or can include non-proton conducting ceramics mixed with metals possessing very high

permeabilities for hydrogen, such as Pd, Nb, Ta, V or Zr. In the case of palladium and its alloys, which possess high permeability for hydrogen as well as good intrinsic catalytic ability for dissociation of molecular hydrogen, a single foil without added catalyst can serve as a dense membrane. To conserve relatively expensive palladium metal, micron thin layers of palladium can be deposited onto screens, porous ceramic, or porous metal supports. The mechanical supports must be made thick enough to resist the desired minimum differential pressure of 3.1 MPa.

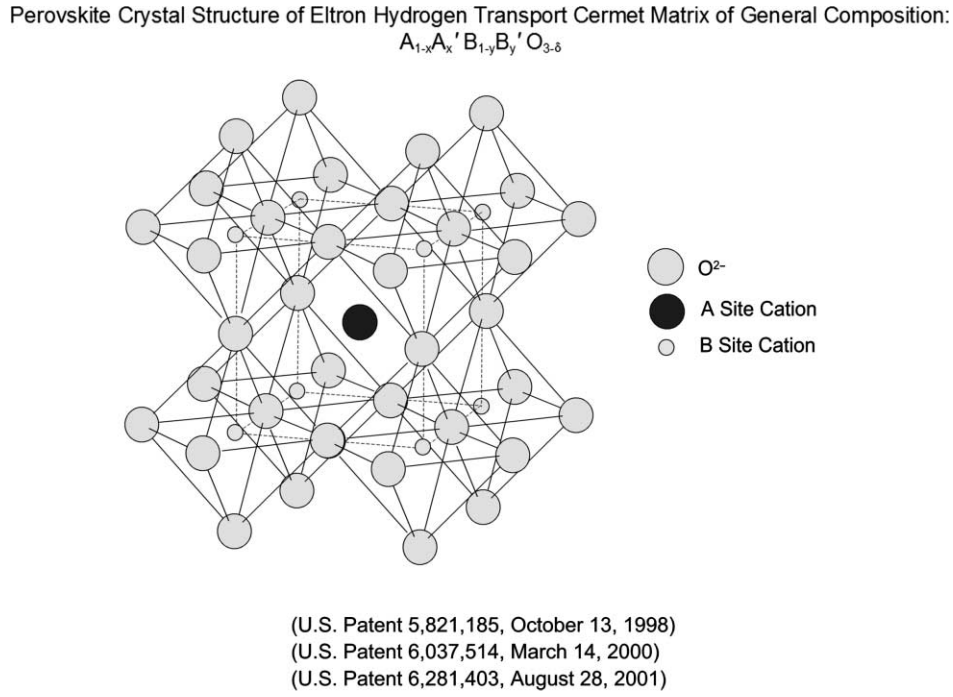

Figure 2: Cubic perovskite crystal structure. Ceramics with this structure are used in proton conducting membranes, palladium cermets, and in porous layers supporting thin layers of palladium.

EXPERIMENTAL

The high pressure measurements were conducted in the apparatus shown in Figure 3, which was designed and built specifically for these studies. The reactor tube was fabricated from a nickel–iron INCONEL alloy. The reactor tube was surrounded by a furnace controlled by a thermocouple placed within the reactor tube and set within a few millimeters of the membrane. The system was designed to operate at a maximum absolute pressure on the hydrogen feed side of the membrane of 3.23 MPa with a differential pressure across the membrane of 3.13 MPa in the temperature range of 613–713 K (which are the temperatures limits of the commercial water gas shift feed and exhaust temperatures [1]). However, most measurements were collected in the upper temperature range of 693–713 K to simulate exhaust temperatures of commercial water gas shift reactors [1]. For measurements of hydrogen flux under ideal conditions, mixtures of dry hydrogen and helium from commercial gas cylinders purchased from AirGas Corporation were fed into the reactor through mass flow controllers purchased from Aalborg, Inc. Helium was used to check for leaks through membranes and seals. Metal membranes were sealed using the copper gasket and flange system described by Peachey et al. [3]. This all-metal sealing system, which is adapted from ultra high vacuum technology, in which leaks are intolerable, was almost invariably leak tight even to helium.

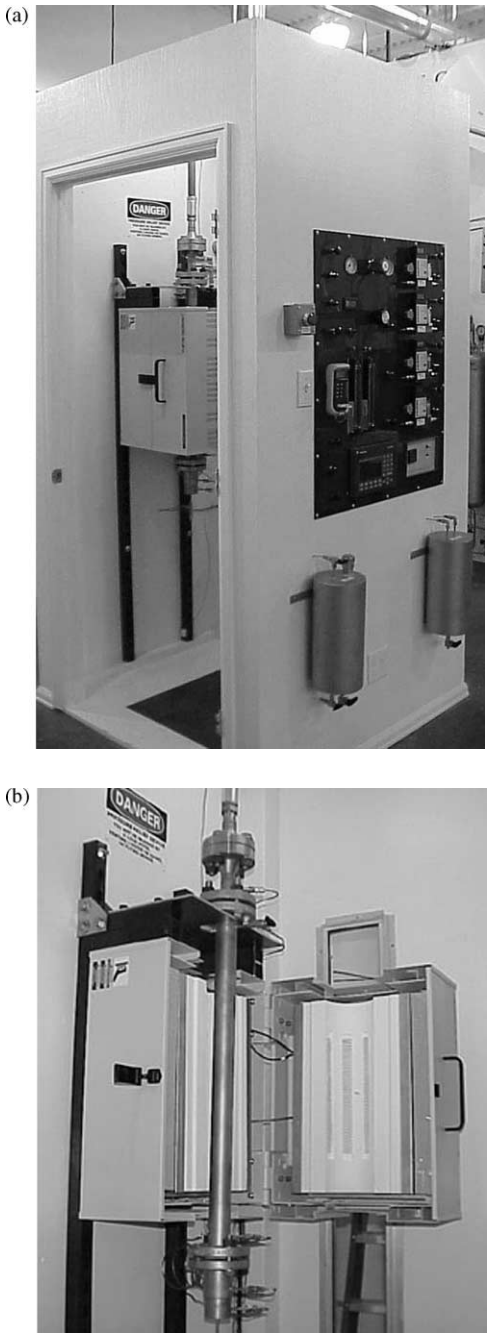

Figure 3: High pressure apparatus used to test membranes. (a) Overview shows gas containment facility. (b) Close-up view showing reactor tube and oven.

Argon or nitrogen at 0.20 MPa was used as the sweep gas. To simulate upstream water gas shift reactor conditions, a mixture of 37.3 mol% steam, 17.8 mol% CO_2, 41.4 mol% H_2, 3.3 mol% CO and balance inert gases was used. A dry mixture of CO_2, CO, H_2 and balance inerts, was purchased pre-mixed from AirGas Corporation, and fed into the reactor through a mass flow controller which was calibrated for the gas mixture using a Precision Scientific Instruments Model 63135 Digital Wet Test Meter, a Ritter Type T61 Drum Type Wet Test Meter and a large bubblemeter, which were compared to one another to ensure accuracy of the primary gas flow calibration. Flow of liquid water was controlled through a liquid mass flow controller and was calculated to produce 37.3 mol% steam when mixed with the dry mixture of CO_2, CO and H_2, plus balance of inert gas. Water was vaporized to steam before entering the reactor.

Gas concentrations in the feeds and exhausts of the permeate and retentate were analyzed by a Shimadzu Gas Chromatograph Model GC-8A. The chromatography apparatus was calibrated using four separate gas mixtures, purchased from AirGas Corporation, containing various concentrations of hydrogen. From the gas concentrations measured by gas chromatography and from the permeate exhaust flow rate determined using a wet test meter, the STP flow rate of hydrogen in the permeate exhaust, and thus the hydrogen flux through the membranes was calculated.

The reactor and reactor oven were surrounded by a gas containment facility (see Figure 3a) which was designed to vent gases and automatically shut off gas flows and to sound alarm in the event of a reactor leak. Carbon monoxide detectors, which are also sensitive to hydrogen, were placed within the containment facility and were used to sound alarm in the event of a leak. The high pressure reactor was also equipped with an internal rupture disk to provide a safety vent to exhaust in the event that pressure design specifications were exceeded.

For metal and metal alloy membranes of Group IVB and VB elements, foils were cleaned by argon sputtering, and palladium catalysts were evaporated in vacuum onto both sides of the foils by methods similar to those described by Peachey et al. [3]. Palladium cermets were fabricated by sintering together palladium and ceramics in air. Cermets of Group IVB–VB elements were fabricated in a vacuum oven to avoid oxidation of the reactive metals. Perovskite ceramics were purchased or synthesized as needed. Thin films of palladium were deposited atop porous layers of ceramic substrates using standard procedures of electroless deposition.

RESULTS AND DISCUSSION

Palladium Membranes

As a control, hydrogen flux was measured through 100 μm thick foils of unalloyed palladium. Figure 4 plots hydrogen flux vs. the difference in the square roots of the hydrogen partial pressures on both sides of the membrane. Data falls fairly well on a straight line. This is in accord with Sieverts' Law, $J = (P_e/l) \times (P_f^{1/2} - P_s^{1/2})$, where J is the hydrogen flux in mol m^{-2} s^{-1}, P_e the permeability at a specific temperature in units of mol m m^{-2} s^{-1} $Pa^{-0.5}$, l the membrane thickness in meters, and P_f and P_s the partial pressures in Pascal of hydrogen on the feed and sink side, respectively. Data following Sieverts' Law is consistent with the usual interpretation that molecular hydrogen dissociates before diffusing through the metal membrane [4].

Figure 5 is an Arrhenius plot constructed by plotting the natural logarithm of the hydrogen permeability in units of mol m m^{-2} s^{-1} $Pa^{-0.5}$ vs. the reciprocal of the absolute temperature. The slope of the line is equal to $-E_{act}/R$, where E_{act} is the activation energy in units of J mol^{-1}, and R the ideal gas constant in units of J mol^{-1} K^{-1}. Data yielded an activation energy for pure palladium of $+15.7$ kJ mol^{-1}. Maximum permeability at 713 K was 1.6×10^{-8} mol m m^{-2} s^{-1} $Pa^{-0.5}$ (as seen from Figure 5 by taking antilog (-17.9)). Activation energies and permeabilities are in good agreement with previous literature values of Refs.[3,5,6]. Using Sieverts' Law to calculate the maximum hydrogen flux which can be expected for a 100 μm (1.0×10^{-4} m) thick palladium membrane (which is assumed to be the minimum required to resist a differential pressure of 3.10 MPa for an unsupported membrane disk, 16 mm in diameter) and assuming a hydrogen feed partial pressure of 1.31 MPa in an upstream water gas shift reactor, and an arbitrary partial pressure of 10,000 Pa on the sweep side of the membrane, the maximum

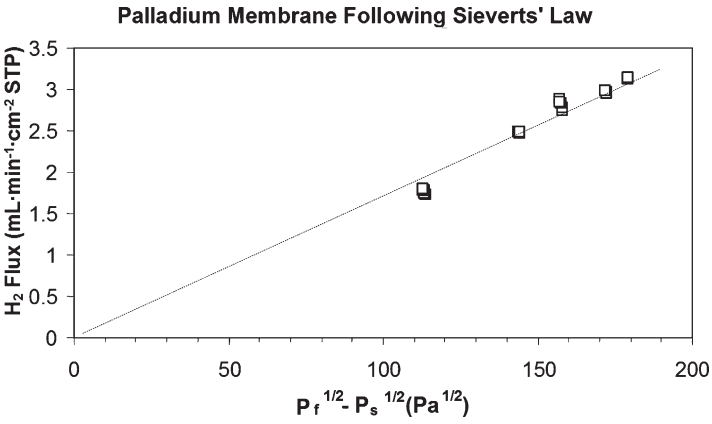

Figure 4: Plot of hydrogen flux vs. difference in the square roots of the hydrogen partial pressures on each side of an unalloyed palladium membrane. Data falls fairly well on a straight line, implying that Sieverts' Law is followed for palladium of 100 μm in thickness.

flux at 713 K will be ($J = 1.6 \times 10^{-8}$ mol m m^{-2} s^{-1} Pa$^{-0.5}$)(1.0×10^{-4} m)$^{-1}$(1,310,000$^{0.5}$ − 10,000$^{0.5}$) = 0.156 mol m^{-2} s^{-1} (21.0 mL min^{-1} cm^{-2} (STP)). However, the cost of pure palladium membranes of 100 μm thick would be prohibitive for a facility such as an electric power plant, for example, attempting to separate 2.0×10^9 kg of CO_2 from 1.8×10^9 kg of H_2 per year, which is the envisioned target goal for commercial membranes.

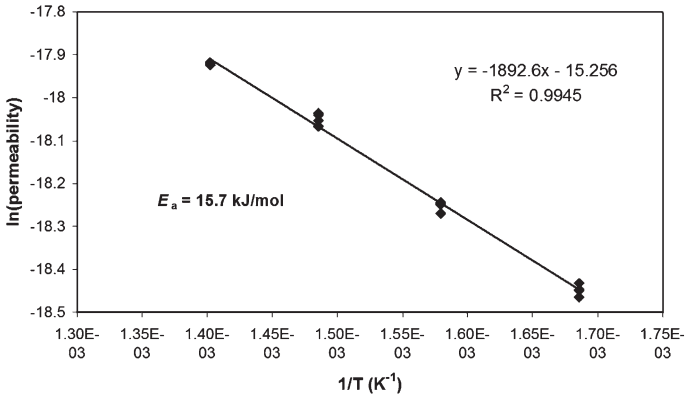

Figure 5: Arrhenius plot of the natural logarithm of hydrogen permeability vs. $1/T$ for an unalloyed palladium membrane, 100 μm thick. From the slope of the line an activation energy of +15.7 kJ mol^{-1} was calculated, in good agreement with literature values. From this Arrhenius plot, permeabilities in the range 593–713 K may be estimated.

Supported Palladium Membranes

According to Sieverts' Law, hydrogen flux is inversely proportional to the membrane thickness, and, in theory, reduction of membrane thickness from 100 to 10 μm, for example, should increase the hydrogen flux tenfold. However, such thin membranes will not withstand differential pressures of 3.10 MPa required

for use in water gas shift reactors without some type of mechanical support. Mechanical supports can include screens and porous layers. Alternatively, palladium can be incorporated into a cermet. It should be noted that Sieverts' Law will break down at membrane thicknesses for which bulk diffusion is no longer the rate limiting step.

In searching for a support which will be compatible with palladium, it is desirable to minimize stress at the palladium substrate interfaces which can lead to the formation of dislocations and cracks. It is also desirable to minimize interdiffusion between palladium and its substrates at the membrane operating temperature, if the membrane is to be stable over time. Dislocations and stress at the interface can be minimized if the crystalline lattices of palladium and its substrate match at the atomic level and if the materials have similar coefficients of thermal expansion over the anticipated temperature range of use and fabrication. Table 1 shows that many ceramics with the cubic perovskite crystal structure match very well with the face centered cubic lattice constants of palladium. Table 2 compares coefficients of thermal expansion of select metals with high permeabilities for hydrogen with select ceramic materials. Defining thermal mismatch as (overlayer−substrate)/(substrate) × 100%, it is preferred that coefficients of thermal expansion match well within 10%, although in practice, mismatches of up to about 30% may be tolerated in some cases. Table 3 lists some select thermal mismatches. Note that mismatches between palladium and alumina (72%), and palladium and titania (54%) are high. Titania and alumina are often used as porous supports for palladium. It should be noted that although some iron−nickel alloys can match thermal expansion coefficients with palladium very well, that some iron−nickel alloys have poor match and that caution should be exercised in assuming that all stainless steels will expand at the same rate as palladium. It should also be noted that these considerations do not take into account possible chemical expansion, which can occur if dissolution of hydrogen causes materials to swell.

TABLE 1
LIST OF SOME SELECT PEROVSKITE COMPOUNDS WHICH MATCH THE CRYSTALLOGRAPHIC LATTICE CONSTANTS OF PALLADIUM AT ROOM TEMPERATURE

Perovskite formula	**Lattice constant Å**	**% Mismatch**
$CaTiO_{3-x}$	3.803	2.3
$GdMnO_{3-x}$	3.82	1.8
$LaCoO_{3-x}$	3.82	1.8
$PrMnO_{3-x}$	3.82	1.8
$La_{0.6}Ca_{0.4}MnO_{3-x}$	3.83	1.6
$CaTiO_{3-x}$	3.853	0.97
$SrFeO_{3-x}$	3.869	0.55
$La_{0.6}Sr_{0.4}MnO_{3-x}$	3.87	0.52
$LaCrO_{3-x}$	3.88	0.26
$LaMnO_{3-x}$	3.88	0.26
$LaFeO_{3-x}$	3.89	0
$SrTiO_{3-x}$	3.893	0
$La_{0.6}Ba_{0.4}MnO_{3-x}$	3.90	−0.25
$BaTiO_{3-x}$	3.98	−2.3

Figure 6 shows cross sections of one of the best porous perovskite materials examined in this study, $LaFe_{0.90}Cr_{0.10}O_{3-x}$, which was used to support 3−4 μm thick layers of dense palladium which was electrolessly deposited atop the perovskite. The $LaFe_{0.90}Cr_{0.10}O_{3-x}$ was chosen because of excellent epitaxial fit between it and palladium, which was predicted to aid initial nucleation and growth, reasonable

TABLE 2
COEFFICIENTS OF THERMAL EXPANSION FOR SELECT MATERIALS

Temp (*K*)	$CaAl_2O_4$	ZrO_2	Ta	Zr	Cr_2O_3	Al_2O_3	Nb	$MgAl_2O_4$	TiO_2
600	6.4	6.7	6.9	7.1	7.8	7.9	8.0	8.4	8.8
700	6.8	6.5	7.1	7.6	7.6	8.2	8.1	9.1 (800)	9.1
1000	7.8	6.9	7.3	8.2	7.3	9.1	8.6	9.8	9.7
1400	8.3 (1300)	11.6	7.7	9.5	7.8	10.1	9.2	10.9	11.1
Temp (*K*)	**V**	**$SrTiO_3$**	**$BaTiO_3$**	**Fe_2O_3**	**MgO**	**Pd**	**Fe_3O_4**	**Fe**	**Ni**
600	10.2	10.9	10.9	12.0	13.3	13.6	14.0	15.1	15.9
700	10.5	11.2	12.1	12.6	14.0	14.1	17.0	15.7	16.4
1000	11.6	12.0	14.7	13.8	15.0	15.6	24.0 (900)	16.6	17.4
1400	13.6	13.3	16.0	14.5	16.0	–	–	23.3 (fcc)	19.5

TABLE 3
THERMAL MISMATCH BETWEEN SELECT MATERIALS

Temp (*K*)	Ta–$CaAl_2O_4$	Ta–ZrO_2	Zr–ZrO_2	Ta–Al_2O_3	Zr–Al_2O_3	Nb–Al_2O_3	Nb–$MgAl_2O_4$
600	7.8	3.0	6.0	−12.7	10.1	1.3	−4.8
700	4.4	9.2	17.0	−13.4	7.3	−1.2	–
1000	−6.4	5.7	18.8	−19.8	9.9	−5.5	−14.0
1400	–	−33.6	18.1	−23.8	5.9	−8.9	−15.6]
Temp (*K*)	**V–Al_2O_3**	**V–$SrTiO_3$**	**Pd–$SrTiO_3$**	**Pd–MgO**	**Fe–Fe_3O_4**	**Pd–Al_2O_3**	**Pd–TiO_2**
600	29.1	6.4	24.8	2.3	7.9	72.2	54.5
700	28.0	6.3	25.9	0.7	7.6	72.0	54.9
1000	27.5	3.3	30.0	4.0	–	71.4	60.8
1400	34.7	2.3	–	–	–	–	–

match of coefficients of thermal expansion, possible water gas shift catalytic activity of the $LaFe_{0.90}Cr_{0.10}O_{3-x}$ and sufficient electron conductivity, which aids reduction of palladium compounds to palladium metal during electroless deposition. The ceramic perovskite support was fabricated in two layers. The top layer, approximately 8 μm thick, (Figure 6b) was composed of sub-micron size particles of $LaFe_{0.90}Cr_{0.10}O_{3-x}$. The top layer was supported by a 400 μm thick layer of coarser particles of the same material with larger pores. The purpose of the fine porous layer was to allow ease of plugging of the pores by palladium and to minimize the necessary thickness of the palladium to no more than 3–4 μm. The purpose of the thicker, coarser, porous layer was to provide mechanical support for resisting the required differential pressure, while minimizing the resistance of gas phase diffusion through the pores. Similar strategy is widely reported in the literature using more conventional bi-porous ceramics such as Al_2O_3. Although deposition of palladium onto the electron conducting perovskite appeared to be more straightforward compared to similar deposition onto insulating ceramics, it was concluded that the hydrogen flux predicted for micron thin layers of palladium would be very difficult to achieve in practice due to gas phase diffusion limitations through the >400 μm thick porous layers needed for mechanical support. In addition, for palladium films 3–4 μm thick, it is expected that effects at the palladium surfaces will limit hydrogen flux, and that the flux predicted by Sieverts' Law for bulk diffusion will not be achieved for these very thin palladium membranes.

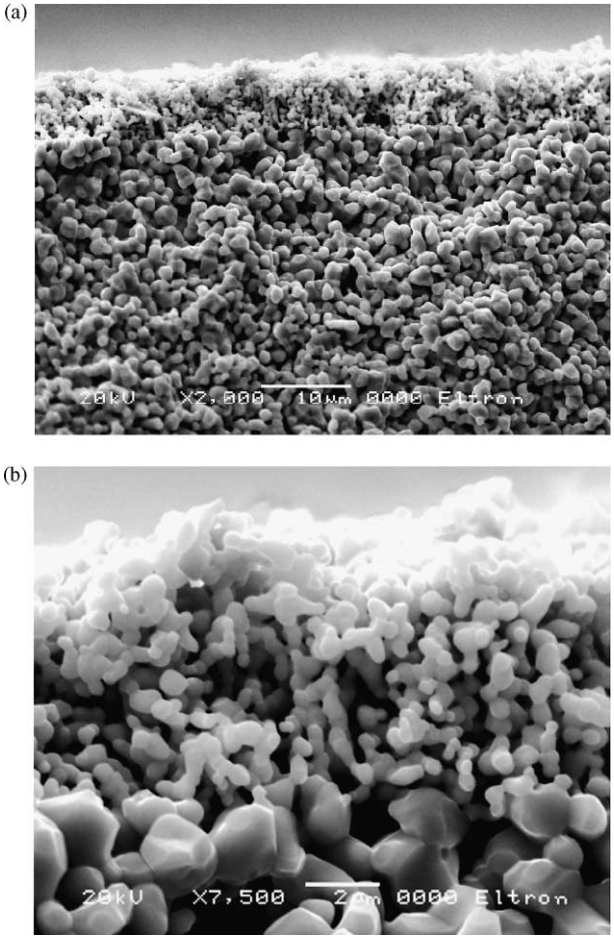

Figure 6: Porous ceramic of $LaFe_{0.90}Cr_{0.10}O_{3-x}$ used to support three to four μm thick layers of electrolessly deposited palladium. (a) 8 μm thick fine porous ceramic layer supported atop a 400 μm thick coarse porous layer. (b) Close-up of fine porous layer atop coarse layer.

Cermet Membranes

Figure 7 shows a cermet which was fabricated by sintering together fine powders of palladium with $LaFe_{0.90}Cr_{0.10}O_{3-x}$. As with the porous supports, materials were chosen for good lattice match, match of coefficient of thermal expansion, and possible water gas shift catalytic activity. Figure 8 shows X-ray powder diffraction data of unalloyed palladium, a cermet of palladium sintered together with $LaFe_{0.90}Cr_{0.10}O_{3-x}$, and the $LaFe_{0.90}Cr_{0.10}O_{3-x}$ powder alone. Overlap of peaks implies similar lattice constants and lattice matching at the atomic level. A permeability of 3.5×10^{-9} mol m m^{-2} s^{-1} $Pa^{0.5}$ was achieved at 723 K, which was less than predicted from a cermet with 40 vol% palladium. The high cost of palladium will likely make the palladium cermets cost prohibitive, even with the mechanical support advantages of the cermets. Cermets of $Nb-Al_2O_3$ and $V-SrTiO_3$ were also fabricated and tested and appeared promising. To protect the metals from oxidation during fabrication at very high temperatures, it was necessary to use a vacuum furnace.

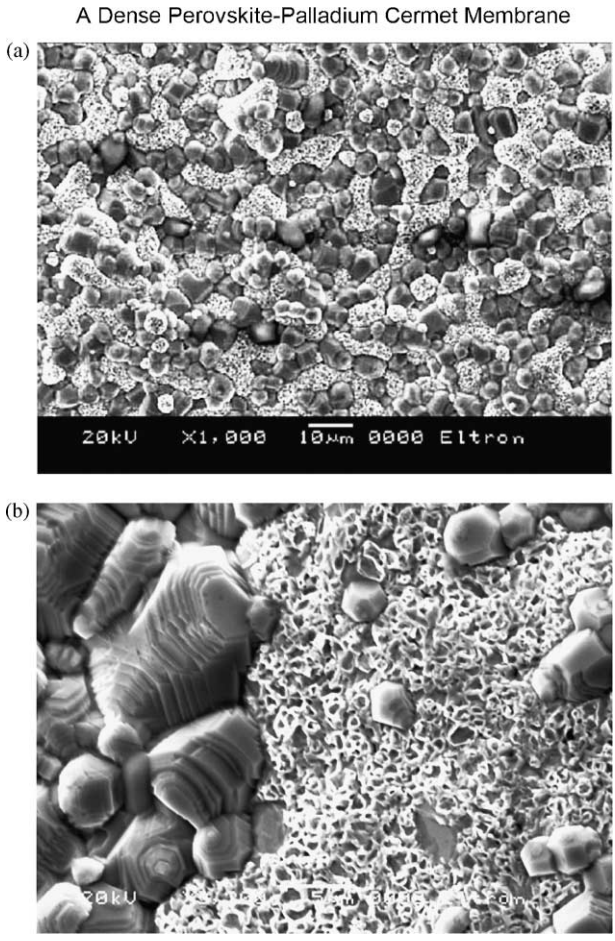

Figure 7: (a) A cermet (ceramic metal) membrane made by sintering together fine powder of palladium and $LaFe_{0.90}Cr_{0.10}O_{3-x}$. (b) Image further magnified. The ceramic phase (dark gray) is on the left and the palladium (light gray) is on the right.

Palladium Coated Group IVB and VB Metal and Metal Alloy Membranes

According to the work of Steward [5] Buxbaum and Marker [6], and Peachey et al. [3], Group IVB and VB elements such as Nb, Ta, V, and Zr are expected to have 10 to 100 times the hydrogen permeability of palladium at temperatures of interest in water gas shift reactors. This implies that membranes of these metals can be 10 to 100 times thicker than palladium and still transport an equivalent hydrogen flux. Greater thickness without loss of hydrogen flux is a great advantage in resisting the required differential pressures and in eliminating pinholes which can plague very thin palladium membranes. The Group IVB and VB elements and their alloys have long been used in the nuclear industry to separate isotopes of hydrogen from helium [7]. They have been touted in the nuclear industry as superpermeable because the membranes are virtually transparent for hydrogen isotopes with energy above 1 eV [8–10]. For use in plasmas, in which hydrogen molecules are dissociated, no catalyst is necessary on the hydrogen source side of the membranes. However, for use in water gas shift

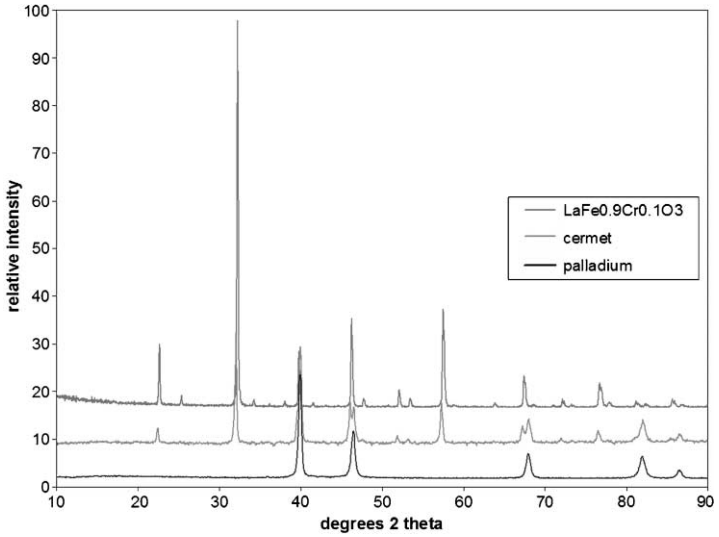

Figure 8: X-ray powder diffraction data (top to bottom) of the perovskite, $LaFe_{0.90}Cr_{0.10}O_{3-x}$, of a cermet of palladium and $LaFe_{0.90}Cr_{0.10}O_{3-x}$, and of unalloyed palladium. Overlap of peaks implies similar lattice constants and lattice matching at the atomic level.

reactors, it is necessary to coat the membranes with hydrogen dissociation catalysts such as palladium. A noble metal such as palladium is also necessary to protect these relatively reactive metals from oxidation by steam and from the formation of carbides and nitrides. Palladium films, only a few hundred nanometers in thickness, coated onto both sides of the membranes are sufficient for protection and for catalysis. Such thin, relatively pinhole-free layers of palladium would be extremely difficult to achieve on porous substrates. Studies of hydrogen flux through some of these materials have been published in Refs. [3,6,11–20]. Unalloyed membranes of Nb, Ta, V, and Zr and a number of their alloys were tested in these studies.

Figure 9 shows hydrogen flux data for dense membranes of four thicknesses which were coated on both sides with sub-micron thick layers of palladium. Data was collected using an ideal hydrogen/helium feed mixture with differential pressures up to 3.1 MPa across the membrane. The thickest membrane (500 μm) followed Sieverts' Law very well, and the data is interpreted that for this thickness of membrane that hydrogen flux is limited by diffusion through the bulk membrane material. The data shows that the permeability of this membrane material was 3.2×10^{-7} mol m m^{-2} s^{-1} Pa$^{-0.5}$ at 713 K. Reducing the membrane thickness in half to 250 μm, doubles the hydrogen flux while the permeability remains constant. This is in accord with Sieverts' Law and implies that hydrogen flux remains limited by diffusion through the bulk membrane material. Some deviation from Sieverts' Law is seen at higher pressures, which is attributed to limitations by gas phase diffusion, as will be subsequently discussed. Upon approximately reducing the thickness in half again to 127 μm, the hydrogen flux no longer doubles as expected from Sieverts' Law implying that a transition has occurred from limitations due to bulk diffusion to some other rate limiting step. Upon further reducing the membrane thickness again to 75 μm, hydrogen flux remains essentially identical to that of the membrane with 127 μm thickness. Because flux did not increase as membrane thickness was reduced, this unambiguously implies that bulk diffusion is not rate limiting for the thinnest membrane, but that surface or interface effects, or other rate limiting steps limit hydrogen flux.

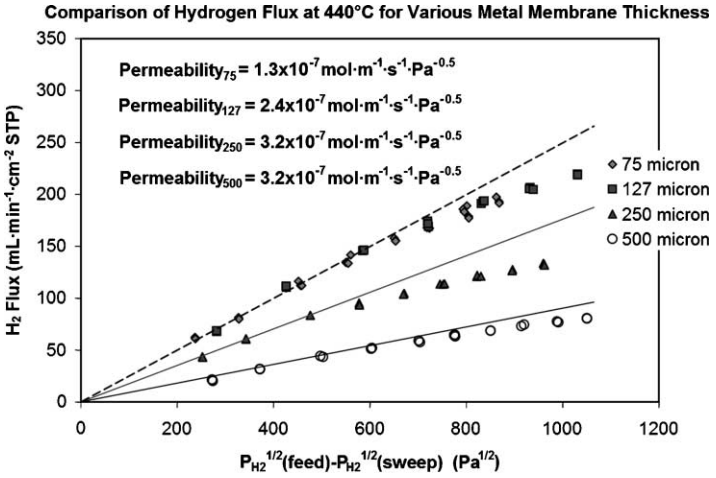

Figure 9: Comparison of hydrogen flux for dense metal membranes of various thickness. Hydrogen flux through membranes 500 and 250 μm thick is limited by bulk diffusion through the membrane material as seen by a doubling of flux when membrane thickness is reduced by half. Hydrogen flux through membranes 127 and 75 μm appears identical, implying that bulk diffusion cannot be rate limiting, but that flux is likely limited by surface or interface effects or some other rate limiting step.

Figure 10a is an Arrhenius plot for a metal membrane 127 μm in thickness, and Figure 10b is an Arrhenius plot for a membrane 250 μm in thickness. The former's slope, yielding an activation energy of $+11.5$ kJ mol^{-1} is positive and near to that of the pure palladium membrane shown in Figure 5, and may imply that the palladium influences the rate limiting step. For the thicker membrane of Figure 10b, the slope is opposite to that of Figure 10a and yields a negative activation energy of -17.7 kJ mol^{-1}. The data of Figure 10b shows that hydrogen permeability decreases through the thicker membranes as temperature increases. This is because the permeability, $P_e = DS$, where D is the diffusivity and S the solubility. Because the solubility of hydrogen in the Group IVB and VB metals decreases at a rate greater than the diffusivity increases, the overall permeability of hydrogen decreases with increasing temperature when the rate limiting step is diffusion through the bulk metal. The data of Figure 10b is consistent with the work of Buxbaum and Marker and Peachey et al. [3,6] who both show decreasing permeability with increasing temperature for metals such as Nb, Ta, V, and Zr. The data of Figure 10 is consistent with the interpretation that hydrogen flux is limited by bulk diffusion through the membrane material for a membrane 250 μm in thickness, but that the rate limiting step changes when the thickness is reduced to 127 μm.

Figure 11 plots hydrogen flux vs. difference in the square roots of the partial pressures of hydrogen on each side of a 127 μm thick membrane of Group IVB–VB material coated with palladium. The data which deviates from the straight line of Sieverts' Law was the same as plotted for the 127 μm thick membrane in Figure 9. The data which deviates from Sieverts' Law used a gas mixture of 60 mol% H_2 and 40 mol% helium. Upon reducing the concentration of helium in the mix, the data seen in Figure 11 again fell on the straight line predicted for Sieverts' Law. This is interpreted as implying that the deviations from Sieverts' Law in the mixture containing 40 mol% helium were due to gas phase diffusion limitations (i.e. hydrogen flux is limited by diffusion of helium away from the membrane to make room for hydrogen). The data of Figure 11 shows that the membrane materials are capable of a hydrogen flux of 280 mL min^{-1} cm^{-2} (STP) (2.1 mol m^{-2} s^{-1}) at 713 K with a partial pressure of hydrogen of 1.37 MPa, if limitations due to gas phase diffusion can be overcome. The data of Figure 11 shows that hydrogen flux may be limited by gas phase diffusion for free standing metal membranes if the metal permeability is extremely high as in the Group IVB

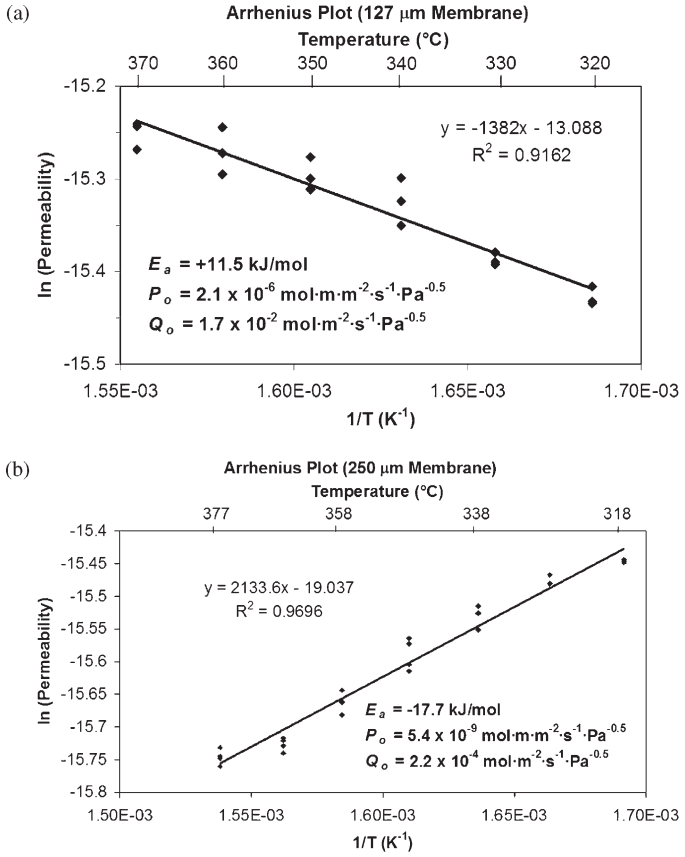

Figure 10: Arrhenius plots for (a) a membrane of a Group IVB–VB material 127 μm in thickness, and (b) a membrane 250 μm in thickness. Data implies that a change in the rate limiting step for hydrogen transport occurs as the membrane thickness is reduced from 250 to 127 μm. Hydrogen flux is limited by bulk diffusion through the Group IVB–VB membrane material for the thicker membrane, but is possibly limited by the palladium catalytic layers for the thinner membrane.

and VB elements and their alloys. This further implies that hydrogen flux through very thin membranes supported by porous layers will almost certainly be limited by gas phase diffusion through stagnant layers of gas trapped in the pores.

Figure 12 plots hydrogen flux using essentially pure hydrogen in the feed to avoid limitations due to gas phase diffusion (helium was used initially to ensure that the seal was leak free). A record flux of 346 mL min^{-1} cm^{-2} (STP) (2.5 mol m^{-2} s^{-1}) was achieved using 2.9 MPa of hydrogen in the feed at 713 K. The data of Figure 12 demonstrates the capabilities of the membrane materials for hydrogen flux when all interference has been removed. These very high flux numbers under ideal conditions are very encouraging for use of these materials in separation of hydrogen from water gas shift mixtures. To overcome limitations due to gas phase diffusion, it was necessary to feed hydrogen to the 2 cm^2 membrane at a rate of 7 L min^{-1} and to use a sweep rate of 4 L min^{-1}. The system was not optimized for turbulent mixing, and design for turbulent mixing will be highly desired for scaled up membrane systems in order to

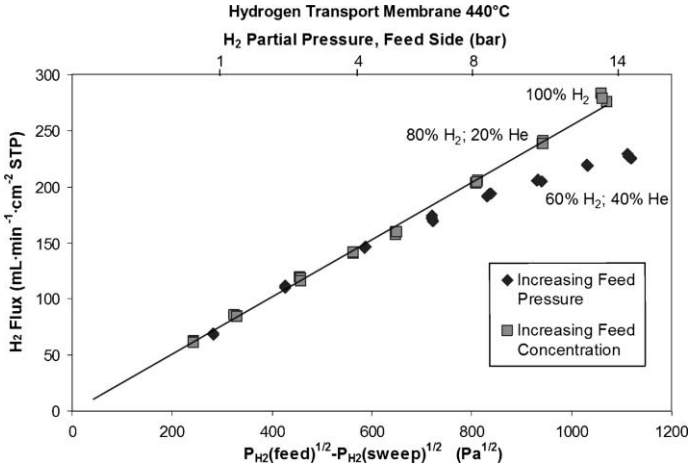

Figure 11: Plot of hydrogen flux for a 60 mol% H_2/40 mol% He mixture showing deviations from Sieverts' Law due to gas phase diffusion limitations, and the removal of the deviations upon reduction of the helium concentration in the gas mixture.

minimize limitations due to gas phase diffusion. For water gas shift mixtures, hydrogen depleted stagnant layers of CO_2 and H_2O near the membrane surfaces limit flux. In order to achieve these record hydrogen fluxes, it was necessary to overcome many obstacles and to overcome many of the rate limiting steps for hydrogen flux.

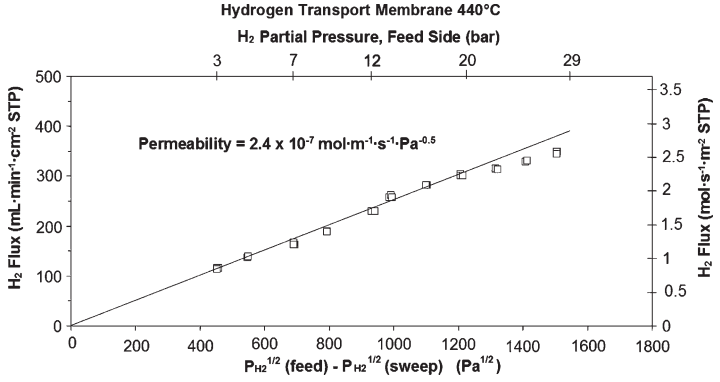

Figure 12: Plot of record hydrogen flux of 346 mL min^{-1} cm^{-2} (STP) (2.5 mol m^{-2} s^{-1}) at 713 using 2.9 MPa partial pressure of hydrogen in the feed.

Care must be exercised in the deposition of the palladium catalysts onto both sides of the membranes. Thick oxide layers and carbonaceous materials must be sufficiently removed before catalyst deposition to avoid formation of diffusion barriers at the palladium–membrane interface. Palladium layers 200–400 nm thick on both sides of the membranes appear sufficient for protection. If catalysts are much over 1 μm in thickness, diffusion will be limited by the catalyst layers. Reactor wall materials

must be carefully selected to avoid hydrothermal transport of materials by steam to the surfaces of the membranes. X-ray photoelectron spectroscopy showed that silicon and sulfur adsorb strongly on the surface of palladium. Considerable H_2S can be released from reduction of the sulfates which are present in fresh commercial water gas shift catalysts of Fe_3O_4. Guard beds of high surface area adsorbents such as $Cu/ZnO/Al_2O_3$ to remove sulfur and high surface area alumina to remove silicon and metals were found to be essential for maintaining membrane catalyst activity for extended periods of time. Because ZnO sinters and loses surface area when heated in steam above about 625 K, improvements in adsorbents or other methods of removing sulfur are desired. Finally, because of the exceptional permeability of the Group IVB–VB membrane materials, limitations due to gas phase diffusion through hydrogen depleted stagnant layers of CO_2 and H_2O need to be overcome. Desorption of CO at 693–713 K appears sufficient to avoid poisoning of the Pd catalysts by CO. Adsorption of steam and CO_2 appear not to interfere with the catalysis at these temperatures. Transport of various impurities by steam from the walls of the reactor to the membrane surfaces appears more critical than the effect of pure steam alone. If H_2S is present in the water gas shift mixture, it is recommended that this be removed by use of adsorbents.

CONCLUSIONS

A variety of dense hydrogen transport membranes, capable of essentially 100% selectivity for separation of H_2, were tested for compatibility with water gas shift reactor conditions. Types of membrane considered included proton conducting ceramic oxides, palladium, micron-thin layers of palladium supported by porous material, cermets fabricated by sintering together powders of metals and ceramics, and composite metal foils of Group IVB–VB metals and their alloys. Select Group IVB–VB elements and their alloys, when appropriately catalyzed and prepared, appear far superior to the other classes of dense membrane under water gas shift reactor conditions. Free standing disks, only 127 μm thick and 16 mm in diameter supported at the rim by metal gaskets were capable of resisting a target differential pressure of 3.1 MPa, and an absolute pressure of 3.2 MPa on the hydrogen feed with a partial pressure of hydrogen of 1.3 MPa. Record hydrogen flux of 2.1 mol m^{-2} s^{-1} at 713 K at the target partial pressure of hydrogen of 1.3 MPa was achieved. A higher flux of 2.5 mol m^{-2} s^{-1} was achieved upon increasing the hydrogen partial pressure to 2.9 MPa. Scaled up versions of such membranes may allow conventional combustion of carbonaceous fuels in air to be replaced by more efficient steam reforming of fuels followed by water gas shift and separation of CO_2 from H_2. Such membranes will allow essentially pure hydrogen to be utilized as a clean fuel, while retaining CO_2 at high pressure and at high concentration, which is desired for economical sequestration.

RECOMMENDATIONS

Membranes fabricated from select Group IVB–VB elements (e.g. niobium, tantalum, vanadium, and zirconium) and their alloys appear suitable for separating H_2 from CO_2 from high pressure water gas shift reactors operating at 693–713 K at reasonable cost. Issues relating to long-term stability and effects of various impurities in the water gas shift gas stream will need to be addressed in future research.

NOMENCLATURE

GC	Gas chromatography
MPa	mega Pascal
mol	mole
STP	Standard temperature and pressure
wt	weight

ACKNOWLEDGEMENTS

The authors would like express their appreciation for the support of David Hyman, the DOE Project Officer on the "CO_2 Capture Project: An Integrated, Collaborative Technology Development Project for Next Generation CO_2 Separation, Capture and Geologic Storage".

This chapter was prepared with the support of the US Department of Energy, under Award No. DE-FC26-01NT41145, and any opinions, findings, conclusions or recommendations expressed herein are those of the author(s) and do not necessarily reflect the views of the DOE.

The following are also acknowledged:

Department of Energy Award DSE-FC26-01NT41145. Adam E. Calihman for high-pressure flux measurements. Alexander J. Gibb for ambient pressure flux measurements.

David A. Gribble, Jr. for deposition of catalysts. Richard Mackay for X-ray analysis. Sara L. Rolfe for synthesis of pervoskites, SEM analysis, formation of cermets and bi-porous ceramic supports. Timothy P. Covino for testing of various composite membranes.

REFERENCES

1. M.V. Twigg, Catalyst Handbook, 2nd ed., Manson Publishing Limited, London, 1997.
2. F.S. Galasso, Structure, Properties and Preparation of Perovskite-Type Compounds, Pergamon Press, Oxford, 1969.
3. N.M. Peachey, R.C. Snow, R.C. Dye, *J. Membr. Sci.* **111** (1996) 123.
4. S.N. Paglieri, J.D. Way, *Sep. Purif. Methods* **31** (2002) 1.
5. Steward, S.A., (1983). *Review of Hydrogen Isoptope Permeability Through Materials, Lawrence Livermore National Laboratory Report UCRL-53441; DE84 007362*. Available from: National Technical Information Service, US Department of Commerce, Springfield, VA, USA.
6. R.E. Buxbaum, T.L. Marker, *J. Membr. Sci.* **85** (1993) 29.
7. J.K. Baird, E.M. Schwartz, *Z. Phys. Chem.* **211** (1999) 47.
8. A.I. Livshits, F. Sube, M.N. Solovyev, M.E. Notkin, M. Bacal, *J. Appl. Phys.* **84** (1998) 2558.
9. A.I. Livshits, M.E. Notkin, M. Bacal, *J. Appl. Phys.* **91** (2002) 4105.
10. A.I. Livshits, V.N. Alimov, M.E. Notkin, M. Bacal, *Appl. Phys. Lett.* **81** (2002) 1.
11. D.J. Edlund, W.A. Pledger, *J. Membr. Sci.* **77** (1993) 255.
12. R.E. Buxbaum, A.B. Kinney, *Ind. Eng. Chem. Res.* **35** (1996) 530.
13. T.S. Moss, N.M. Peachey, R.C. Snow, R.C. Dye, *Int. J. Hydrogen Energy* **23** (1998) 99.
14. S. Hara, N. Hatakeyama, N. Itoh, H.-M. Kimura, I. Inoue, *Desalination* **144** (2002) 115.
15. Y. Zhang, T. Ozaki, M. Komaki, C. Nishimura, *Scripta Materialia* **47** (2002) 601.
16. C. Nishimura, M. Komaki, M. Amano, *Mater. Trans. Jap Inst. Met.* **32** (1991) 501.
17. C. Nishimura, M. Komaki, M. Amano, *Trans. Mat. Res. Soc. Jpn* **18B** (1994) 1273.
18. C. Nishimura, M. Komaki, M. Amano, *J. Alloys Compounds* **293–295** (1999) 329.
19. C. Nishimura, M. Komaki, S. Hwang, M. Amano, *J. Alloys Compounds* **330–332** (2002) 902.
20. T. Ozaki, Y. Zhang, M. Komaki, C. Nishimura, *Int. J. Hydrogen Energy* **28** (2002) 297.
21. T. Ozaki, Y. Zhang, M. Komaki, C. Nishimura, *Int. J. Hydrogen Energy* **28** (2003) 1129.